Optimizing the design of silica coating for productivity gains during the TIG welding of a 304L stainless steel

Guillaume Rückert, Bertrand Huneau, Surendar Marya

Optimizing the design of silica coating for productivity gains during the TIG welding of 304L stainless steel

G. Rückert *, B. Huneau, S. Marya

Institute Gem-UMR CNRS 6183, Ecole centrale de nantes, 1 rue de la Noe, BP 92101, 44321 Nantes Cedex, France

The performance of silica coatings on TIG (or GTA) welding of AISI304L stainless steel has been studied by investigating the effect of coating geometry and thickness on weld penetrations. Two coating designs are studied. One involves a 20 mm wide continuous coating across the weld zone and the second design formulates two parallel coatings 1–7 mm apart around the joint. The optimum thickness for continuous coatings is limited to about 50 μm whereas for 2 mm apart coatings, the optimum range extends from 70 to 200 μm. The presence of a narrow bare zone in the coating is suggested to be more practical for manual silica application. Tensile tests have been performed to identify the mechanical behavior in different characteristic zones of the welded specimens. The reduced tensile strength of the weld metal is attributed to the flux silica particles.

Keywords: Ferrous metals and alloys; Welding; TIG; Silica coating

1. Introduction

The welding industry has a long practice of fluxes designed to improve arc stability, weld cosmetics and performance by protecting the weld pool from undesirable ambient reactions [1]. Fluxes have also been designated to modify weld pool chemistry by slag-melt reactions with specific aim of improving the weld service behavior. The flux application for TIG (also called GTA) welding, although dating back to early sixties [2,3], is drawing further attention in recent years from researchers prompt to investigate how weld pool dynamics and arc profiles are affected by additives on elements present in flux coatings. In fact, the application of some flux coatings have been found to increase interestingly the weld penetration, though the legendary weld cosmetic of TIG welds may somewhat be degraded. By the mere application of some flux coatings, Activated-TIG (A-TIG) process generates 6–8 mm penetrations in one single pass for most of the commonly welded alloys. This is about twice the weld penetration in conventional TIG process without flux [4–6]. Various mechanisms have been proposed to explain the improvement in weld penetration; arc constriction [7] and weld pool melt inversion [8,9]. The arc constriction is thought to result principally from two phenomena:

- the presence of ionized flux elements that modify the charge distribution towards the central region of the arc [7];
- the creation of flux denuded central region directly under the electrode subsequent to flux vaporization. The central zone then becomes more conducting than the outer regions where flux, molten or not, offers higher resistance to current flow. In fact, silica (SiO_2) is very resistive and becomes increasingly conducting with temperature in the molten phase. The flux vaporization in the central part of the arc increases electron channeling and is thought to reduce the anode spot size [10].

The nature and exact composition of flux coating depends on the material to be welded (Table 1). For plain

* Corresponding author. Tel.: +33 2 40 37 16 36; fax: +33 2 40 37 16 72.
E-mail address: surendar.marya@ec-nantes.fr (S. Marya).

Table 1
Common activating fluxes for carbon and stainless steels welding

Materials	Activating fluxes
Plain carbon steels	SiO_2 [3; 14; 15; 16], TiO_2 [3; 16], Cr_2O_3 [3; 16], NaF [3], Ti [3]
Stainless steels	SiO_2 [17; 18; 19; 20; 21], CaF_2 [17], AlF_3 [17; 21], TiO_2 [17; 18; 22; 23; 19; 20; 20], Fe_2O_3 [17], Al_2O_3 [17], Cr_2O_3 [20], CaO [20], MgO [20], ZrO_2 [20]

carbon and stainless steels, as mono component flux, silica has very often been selected for its positive contribution to weld penetration. However, the generation of a homogeneous flux coating remains problematic because flux is still applied manually. Over a long run, the weld becomes irregular due to inconsistent coating thickness. The first aim of this study is thus to define a window of thickness range over which weld results remain constant. Moreover, silica is also employed in a new technique called Flux Bounded-TIG to weld aluminum alloys in alternating current (AC) [10,11]. The flux in FB-TIG is applied not as a single cover, but as a set of two parallel coatings, x mm apart (Fig. 1b). Electrical resistivity of the flux is supposed to channel the incoming electrons onto the central metallic zone exempt from the flux coating. In case of aluminum alloys, weld penetrations of 6 mm and more during AC welding have been reported by the application of two narrowly separated silica coatings [10]. In fact, without a narrow uncovered zone in between the coatings, the AC arc becomes erratic. The concept of two separate coatings is also attractive from perspectives of flux consumption if weld penetrations comparable to A-TIG can be obtained over a broad range of coating thickness. To the authors knowledge, no such work has so far been reported on stainless steels. The objective of the present investigations is also to check this action and to compare penetration depths obtained in A-TIG and FB-TIG coating configurations.

2. Experimental

Bead-on-plate welds are carried out on AISI304L stainless steel with or without coating applied by manual application of a silica paste. Principal process parameters are listed in Table 2 and Fig. 1 shows the coating design. In subsequent discussion, continuous coatings are designated as A-TIG with reference to literature practice and separated coatings as FB-TIG [10].

Table 2
Experimental conditions

Parameters	Values	Units
Material	AISI 304L	
Sheets dimensions	$200 \times 80 \times 6$	mm
Bead length	100–130	mm
Welding current	100–125–150	A
Welding speed	125	mm/min
Arc length	2	mm
Electrode	$W + 2\%$ ThO_2	
Diameter of Electrode	2.4	mm
Tip angle	60	
Shielding gas flow (Argon)	12	l/min

For A-TIG and FB-TIG process, a paste is obtained by mixing silica powder in a liquid carrier which is very often alcohol or acetone. However, such volatile solvents do not allow to maintain a constant liquid/silica concentration in flux paste. Thus in order to ensure a constant mass application, distilled water was preferentially used as liquid carrier. In the present study, silica is not dissolved in distilled water but remains as suspension to constitute a silica gel. The flux coating is then made by a brush dipped in the silica water paste. After drying, silica particle size is measured (Fig. 2a) and compared to acetone assisted coating (Fig. 2b). The distilled water assisted coating is regular with fine particles, while acetone liquid carrier paste produced large particle clusters of 50–60 μm after drying.

In FB-TIG configuration, two separated coatings are applied. The gap between coatings (x, mm) varies from 0 to 7 mm. In fact, $x = 0$ mm corresponds to A-TIG welding. The height of generated silica coating is controlled by positioning the focus of optical microscope with an accuracy of a few microns. According to mass of flux in water (W_p in %), coating thickness (t in mm) after drying varies linearly as indicated in Fig. 3. It is difficult to have a coating less than 10 μm thick due to the particle size which is close to 10 μm (Fig. 2a).

Metallographic specimens are prepared by polishing followed by etching in nitric acid (50%) during 30 s. Melt-cross sections are observed with stereo microscope to measure penetration depth (D in mm) and width (W in mm). Arc voltage (U in V) and video acquisition with a CCD Camera during welding tests generate further information on the process and complete geometrical measurements.

3. Results and discussion

3.1. Influence of coating thickness

The coating thickness is observed to have a very profound effect on weld penetration (Figs. 4 and 5). The weld penetration first increases linearly with coating thickness up to 50–70 μm and subsequently shows declining trend (Fig. 4). TIG weld penetrations correspond to zero coating

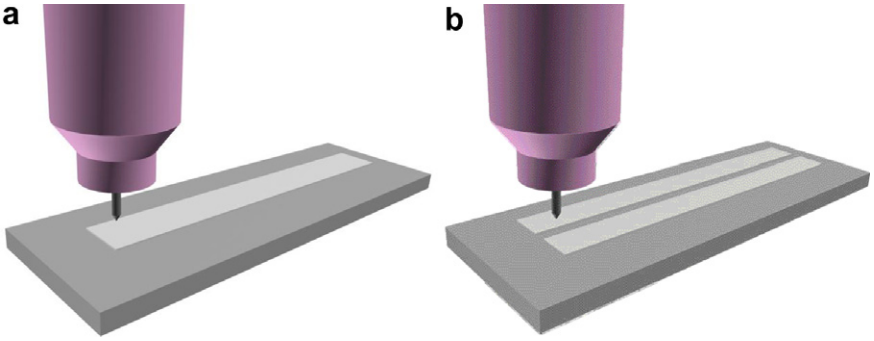

Fig. 1. Schematic diagram of flux application in A-TIG (a) and FB-TIG (b) configurations.

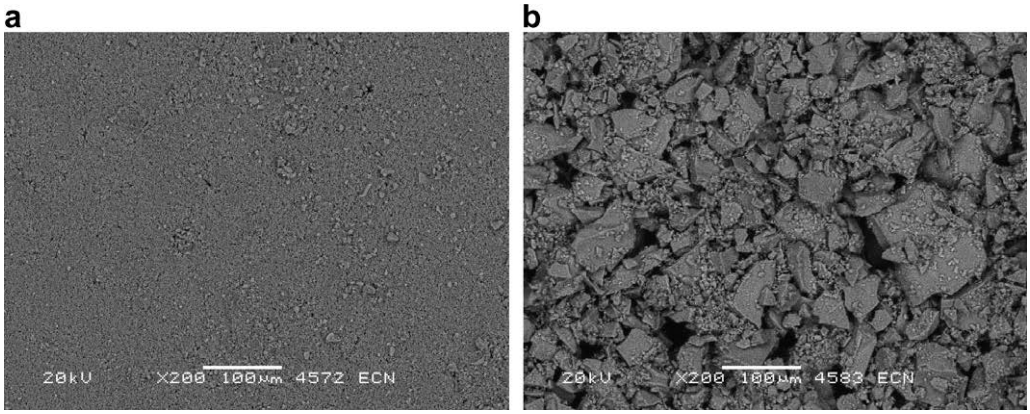

Fig. 2. Observations on distilled water (a) and acetone assisted silica coatings (b) under SEM.

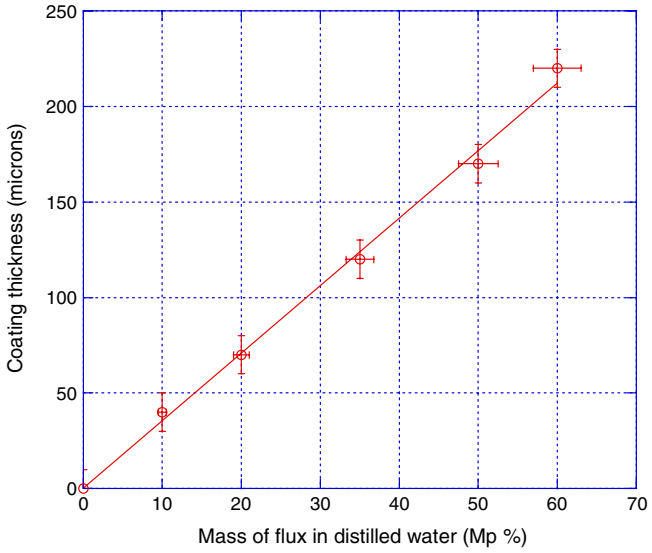

Fig. 3. Evolution of the coating thickness with the mass of flux in distilled water.

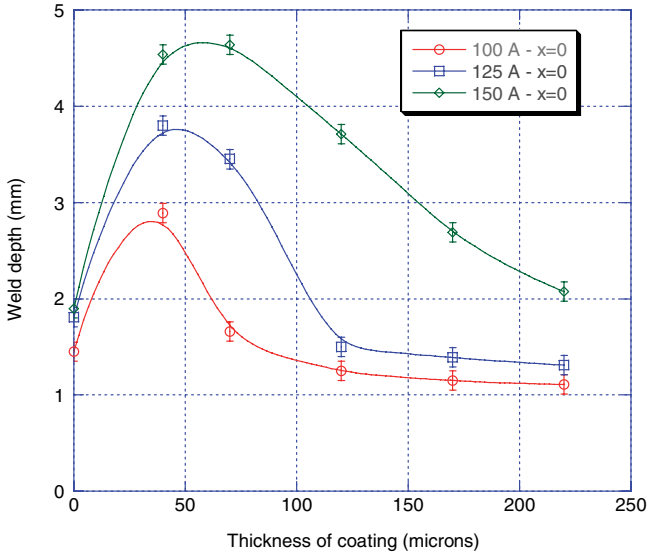

Fig. 4. Evolution of penetration depths with coating thickness in A-TIG welding.

thickness and ranges from 1.4 to 1.9 mm for the investigated welding currents of 100 to 150 A. Depending on the welding current, the maximum of penetration in A-TIG, depending on the current, is obtained for the coating thickness ranging between 40 and 70 µm. The observed maximum values of weld penetration are 4.8 mm, 3.9 mm and 2.9 mm respectively for the welding currents of 150, 125 and 100 A. The optimal thickness seems to increase with the welding current. For example, maximum of penetration is obtained around 40 µm at 100 A and around 70 µm at 150 A. The optimization of the coating thickness thus depends on the incident energy.

Beyond the optimal thickness, weld penetrations decrease significantly. This rapid fall can be explained by higher energy consumption required to break the flux barrier. In fact, silica is non conducting and offers high electrical impedance to the arc. A stable arc is established only when the flux becomes liquid or completely removed through vaporization. As the amount of energy consumption for this effect increases with the thickness of the coating, the part of incident energy effectively used to create the weld pool is strongly reduced.

Further, as the coating thickness increases, the electric arc is impeded by non molten flux offering higher electrical impedance on the advancing side. This induces modification in arc profile which is then stretched backwards on to the molten pool (Fig. 5c). This trailing effect is all the more important with increasing coating thickness for a given current or for a given thickness with reductions in welding currents. Even at the optimal coating thickness around 50 µm (Fig. 5b), the trailing effect exists when video stills from TIG and A-TIG are compared [12]. The trailing effect is related to the higher electrical resistivity of silica which decreases with increasing temperature, particularly when silica changes to the liquid phase. As melting is at higher temperature on the trailing side, arc tends to lag behind the advancing electrode tip. The said arc trailing increases the effective length and partially contributes to voltage increase with coating as reported later in this paper.

In FB-TIG configuration, the evolution of weld penetration is quite similar to that reported above for A-TIG,

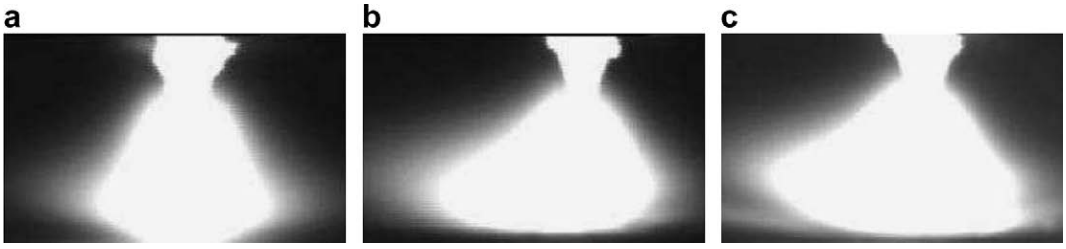

Fig. 5. Arc side views in TIG welding (a) A-TIG welding ($t = 50$ μm) (b) and A-TIG welding ($t = 220$ μm) (c).

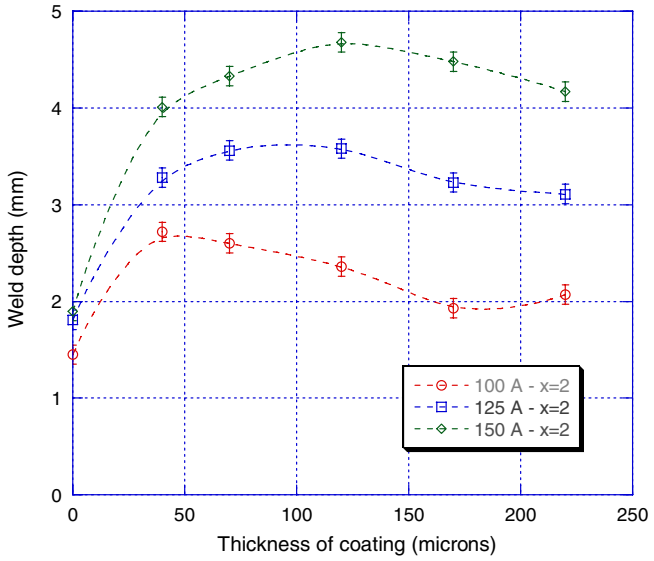

Fig. 6. Evolution of penetration depths with coating thickness in FB-TIG welding.

though the trend is slightly less significant (Fig. 6). For coating thickness corresponding to maximum weld penetrations obtained in A-TIG, the FB-TIG penetration values are weaker. For example, at 150 A with a 50 μm thick coating, A-TIG penetration depth is 4.5 mm compared to 4.0 mm in FB-TIG.

However, comparable penetrations appear in FB-TIG but for higher coating thickness. For example at 150 A, the maximum penetration is obtained with a 120 μm thick coating in FB-TIG compared to 50 μm in A-TIG and the weld penetrations are quite close. Beyond the optimum coating thickness, just as in A-TIG, the penetration decreases with increasing thickness but at a very lower pace in FB-TIG. In the latter process, the presence of the uncovered zone between the two parallel flux strips greatly facilitates the fixation of the anodic spot and arc stability even at lower currents. This is confirmed by the arc voltage results presented in Figs. 7 and 8, which show that voltage surge in FB-TIG remains limited to 0.5 to 1 V, compared to 1 to 2 V for A-TIG.

For a given coating thickness, the voltage jump is inversely related to the welding current and increases with thickness as shown in Fig. 8. For example, the voltage increase for 40 μm coating in A-TIG is 2.3 V at 100 A and 1.5 V at 150 A. Similarly, at 100 A, the voltage increase jumps from

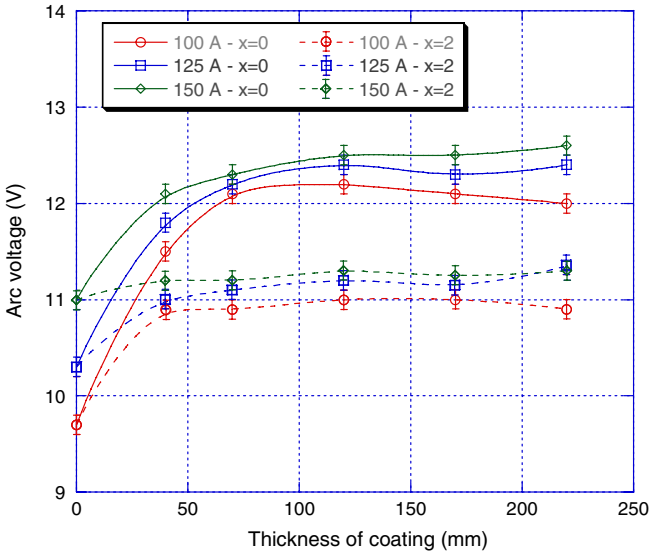

Fig. 7. Evolution of arc voltage with coating thickness in A-TIG (continuous line) and FB-TIG configuration (discontinuous line).

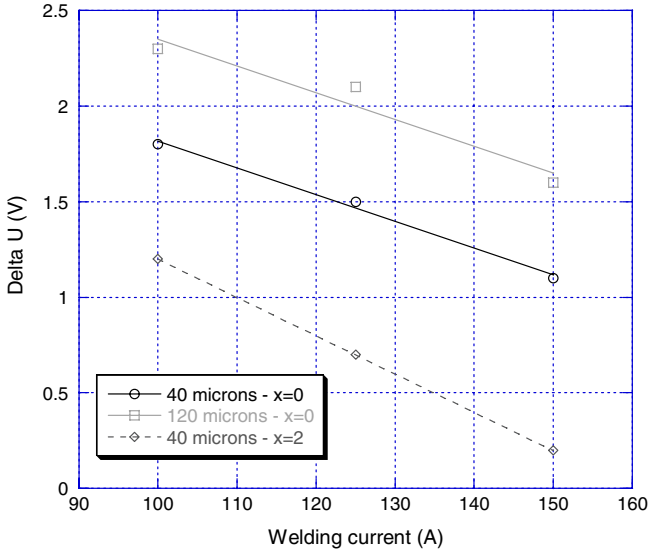

Fig. 8. Arc voltage increase during A-TIG and FB-TIG welding for different coating thickness.

1.6 to 2.3 V when the coating thickness passes from 40 to 220 μm. The effect of decreasing current or increasing thickness on voltage increase in A-TIG are in line with the fact that flux is resistive [13]. Higher is the coating

thickness, bigger is the barrier to electron conduction and the arc voltage consequently increases to maintain equilibrium. With increasing current, the coating barrier is fast overcome subsequent to rapid melting and results in lower voltage surge as shown in Fig. 8. Moreover, whereas the voltage tends to increase slightly with the coating thickness in A-TIG, it remains almost constant in the coating thickness range of 40–220 μm in case of the FB-TIG process (Fig. 7). Whatever the coating configuration, A-TIG or FB-TIG, voltage modifications are important in the initial stages of the flux application, which produces significant increases in weld penetrations as shown in Figs. 4 and 6.

The correlation of penetration depths with the monitored arc voltages does not allow to affirm any direct linkage between them. Indeed, in case of 150 A tests, voltage increase of about 1.2 V in A-TIG and 0.3 V in FB-TIG lead to identical weld penetrations. The electrical data thus does not allow to establish a sufficiently relevant criterion to identify the flux characteristics. From theoretical considerations, as voltage increase implies higher energy, it is tempting to assert greater weld volumes and penetrations. Although the weld pool volumes may increase with arc energy, the weld depth may not. It may even be reduced depending on the weld pool dynamics that are known to be affected by surface tension temperature gradients and energy distribution in the welding arc. From voltage standpoint, FB-TIG with a slight increase in voltage (0.3 V), generates deeper penetrations compared to A-TIG. This suggests that FB-TIG has a higher process efficiency from energy point of view.

From basic theoretical considerations, the difference between A-TIG and FB-TIG weld bead characteristics is expected to depend on the size of the weld pool. Whenever the width of the pool is smaller than the gap x in FB-TIG, a major part of the flux remains out of the electric arc. Only a small part may undergo some changes due to heating of the base plate. The two separate flux coatings of FB-TIG with high electrical impedance are there to channel the electrical arc on to the narrow uncovered base plate. This is supposed to confine the arc and make it more hot in its central part. As such, it is anticipated that without any direct participation of flux, weld penetrations should increase in FB-TIG. However as the weld pool increases beyond the coating gap, flux would be injected into the weld pool and into the arc just as in A-TIG process, though the overall flux content is expected to remain relatively low. In A-TIG process, before arc is channeled, the coating in the central zone has to be melted which requires an expense of energy unavailable for the weld pool creation. This probably explains why FB-TIG has a high energy efficiency from penetration point of view. Arc energy is not used in any way to create a conducting channel in FB-TIG, whereas it is in A-TIG. It thus seems that A-TIG and FB-TIG processes would become closer with increasing weld heat inputs. The results on weld penetration in the region of optimum coating thickness invariably show a better performance with A-TIG. Equivalent weld penetrations, as mentioned earlier, are also obtained in case of FB-TIG but with higher coating thickness. This suggests that it may be possible to determine equivalence of flux volumes consumed in A-TIG and FB-TIG according to the schematic cross-section presented in Fig. 9.

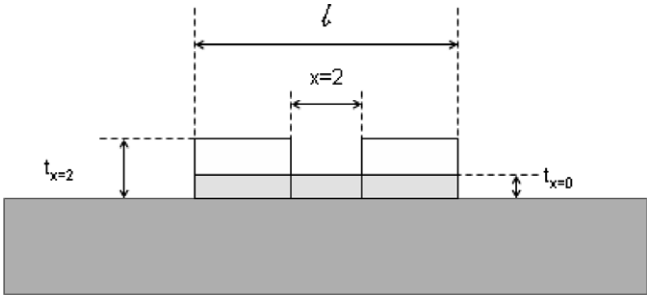

Fig. 9. Schematic cross-section of A-TIG and FB-TIG flux coatings.

For a cross-section, the following relation holds

$$w.t_{\mathrm{ATIG}} = (w - x).t_{\mathrm{FBTIG}} \tag{1}$$

with

- w: width to be defined
- t_{ATIG} and t_{FBTIG}: respective optimal thicknesses for ATIG and FBTIG
- x: gap between coatings of flux for FBTIG configuration

$$w = \frac{(x.t_{\mathrm{FBTIG}})}{(t_{\mathrm{FBTIG}} - t_{\mathrm{ATIG}})} \tag{2}$$

From the experimental results relevant to identical penetration observed at 150 A ($x = 2$ mm, $t_{\mathrm{A-TIG}} = 0.05$ mm and $t_{\mathrm{FB-TIG}} = 0.12$ mm), the width W is evaluated around 3.4 mm which is roughly the size of the anodic spot. The observation of the solidified weld bead shows complete absence of flux slag in the central region of the weld. The outer regions of the weld are however covered with thin layer of a vitrified slag. This suggests that flux is molten and vaporized only in the central part of the weld pool directly beneath the electrode tip. It thus seems that in case of the stainless steel with silica coating, the physical phenomena which contributes to increase the weld penetration are quite similar in A-TIG and FB-TIG with 2 mm coating separation. From the coating width of 3.4 mm, a flux consumption of 0.17 mm^3/mm of weld is estimated for the optimized weld penetration at 150 A.

3.2. Effect of gap between coatings: x

In the first part, devoted to study the effect of coating thickness on weld penetrations, the FB-TIG spacing between flux coatings was fixed at 2 mm. This value chosen empirically is about the half the size of the anodic spot. The difference of results in both A-TIG ($x = 0$ mm) and FB-TIG ($x = 2$ mm) configurations highlights the great influence of this parameter. Fig. 10 illustrates penetration depth and monitored arc voltage variations with x(mm) for a

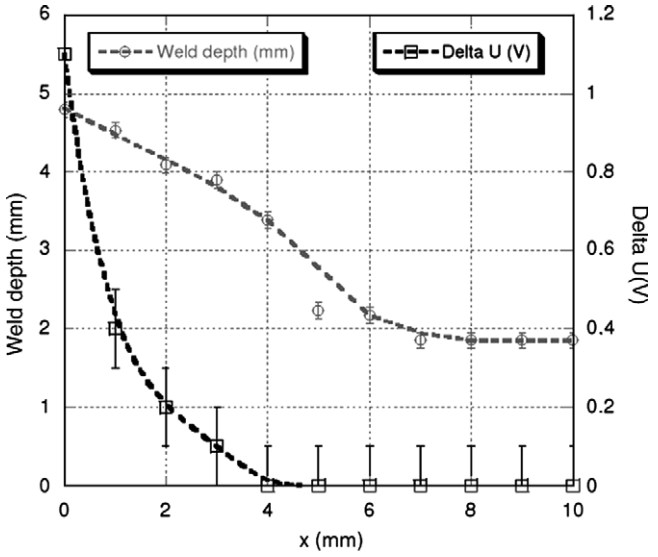

Fig. 10. Evolution of weld depth and arc voltage with gap (x) between coatings.

50 μm thick optimized silica coating. The penetration curve breaks down into two distinct parts:

- when the x spacing between the flux coatings is greater than the expected width of the TIG weld pool under the given processing parameters, flux does not have any effect. As expected, arc voltage in TIG and FB-TIG are very close, as flux coating is remote from the weld pool.
- as x is progressively reduced and becomes smaller than the width of the weld pool, the flux contributes to its formation via the weld pool and the arc. Between $x = 4$ mm and $x = 0$ mm, both arc voltage and weld penetrations increase with the contracting of x. The increasing arc voltage suggests that elements from flux intervene to modify the prevailing charge carrier distribution in the arc. In addition, arc views perpendicular to the welding direction show a stretching of the arc on the rear side of the weld pool. However, between $x = 0$ mm and $x = 1$ mm, the abrupt increase in voltage is awarded by only a slight increase in penetration. Arc trailing is observed as in A-TIG particularly as the gap between the coatings is reduced. This does positively contribute to arc voltage rise through increased arc length.

3.3. Weld metal characterization

Silica application that enhances weld penetration is also expected to modify the weld metal chemistry and mechanical characteristics. To determine the extension of modifications, weld metal was characterized in its cross-section for possible silica based inclusions and tensile tests were carried out by using digital image correlation technique. This generated tensile behavior of heat affected and weld metal zones in a single test condition.

Preliminary observations by optical microscopy revealed a homogeneous distribution of 1–2 μm inclusions with an approximate density of 3400 inclusions/mm^2. The Energy Dispersive Spectrometry of X-rays (EDSX) showed that inclusions combine silicon, oxygen and manganese. The exact quantification of oxygen was difficult, but inclusions are identified to combine silicon to manganese m_{Si}/m_{Mn} ratio of 3/4. The stainless steel does contain 0.32% Si and 1.79% Mn, but higher inclusion density combined with higher silicon to manganese ratio in the weld bead can only be explained by absorption of silica flux by the weld pool.

The summarized characteristics of the tensile tests (Table 3) reveal that the weld metal in A-TIG undergoes localized necking beyond the tensile strain of 22% and its tensile strength is reduced by about 50 MPa compared to

Table 3
Mechanical properties in different domains of the welded structure

	WZ (TIG)	HAZ (TIG)	WZ (A-TIG)	HAZ (A-TIG)
Yield strength (MPa)	344	344	339	335
Ultimate tensile strength (MPa)	635	>635	585	>585

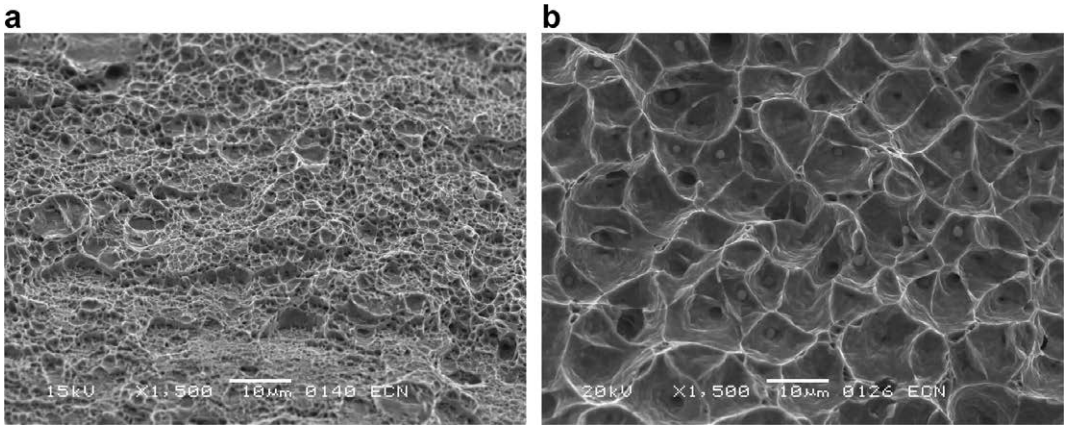

Fig. 11. Fracture topography in TIG welded zone (a) and A-TIG welded zone (b) observed under SEM.

TIG welds. The specimens always break in the weld metal. Moreover the base metal tensile strength is hardly affected by TIG welding. The reduction in tensile strength of A-TIG welds can be attributed to higher inclusion density as suggested by observation of the fractured surfaces under the scanning electron microscope (Fig. 11). A-TIG weld metal reveals large size dimples centered around the observed inclusions. Base metal and conventional TIG weld metals reveal fine dimpled structures and comparatively higher elongations.

4. Conclusions

The present study investigates the design of flux application by defining the silica coating geometry and lays out that leads to the optimized flux performance for the fusion welding of stainless steels using the conventional TIG welding process. The principal results may be summarized as follows:

- the silica water mixture allows to obtain precisely determined coating thickness. After drying, the coating is characterized by very fine silica particles when water is used as liquid carrier. Acetone or alcohol though more easy to eliminate produce large size particles and coating thickness is difficult to control.
- the coating thickness is an essential parameter in A-TIG welding. It is generally recommended not to exceed 200 μm without comments on how welding energy might affect the thickness-penetration results. This study shows significant variations in weld penetration in 0–200 μm range. The optimized thickness in A-TIG is observed to vary between 40 and 70 μm depending on the welding current. At optimized thickness, the coating doubles the weld penetration at a given current level. For further increase in coating thickness, the overall performance in terms of weld penetration is reduced. In A-TIG, coating thickness window is very narrow. FB-TIG configuration allows to obtain comparable results for thicker deposits with enlarged range of coating thickness. The sensitivity of weld penetration with coating thickness is thus reduced in FB-TIG.
- the silica application generates higher inclusion density in weld metal with resulting decrease in the tensile strength. However, this reduction is comparatively weak when improvement in weld penetrations are considered in overall process analysis.
- this optimization of parameters is the first step for the automation of the coating application in order to promote industrial applications.

References

[1] Olson D, Liu S, Frost R, Edwards G, Fleming D, Welding brazing and soldering, ASM handbook edition, vol. 6, 1993, Ch. Nature and behavior of fluxes used for welding, p. 55–63.

[2] Lucas W, Howse D. Activating flux – increasing the performance and productivity of the TIG and plasma processes. Weld Met Fabr 1996;64(1):5.

[3] Lucas W, Howse D, Savistky M, Kovalenko I. A-TIG flux for increasing the performance and productivity of welding processes. In: IIW/IIS Budapest proceedings, IIW Commission XII, Budapest, Romania. 1996. p. 257–74.

[4] Gurevitch S, Zamkov V, Kushnirenko N. Improving the penetration of titanium alloys when they are welded by argon tungsten arc process. Avt Svarka 1965(9):1–4.

[5] Paskell C, Lundin T, Castner H. GTAW flux increases weld joint penetration. Welding Journal 1997:57–62.

[6] Savitskii M, Kushnirenko B, Lupan A. Special features of the formation of welds made with activating fluxes. Automat Weld 1981;34(2):23–5.

[7] Simonik A. Effect of contraction of the arc discharge upon the introduction of electro-negative elements. Svar Proiz 1976(3):68–71.

[8] Heiple C, Roper J. Mechanism for minor element effect on gta fusion zone geometry. Weld J, Welding Research Supplement, 1982.

[9] Marya S, Olson D. Effect of minor elements and process parameters on gta weld bead variances in steels. Mémoires et Etudes Scientifiques – Revue de Métallurgie, 1989. p. 25–34.

[10] Sire S, Marya S. On the development of a New Flux Bounded TIG process (FBTIG) to enhance weld penetrations in aluminium 5086. Int J Form Proc 2002;5(1):39–51.

[11] Sire S, Ruckert G, Marya S. Flux optimisation for enhanced weld penetration in aluminium contribution to FBTIG process. Weld World, Le Soudage Dans Le Monde 2002;46(SPEC):207–17.

[12] Middel W, Pieters R, Den Ouden G. Influence of additives on arc properties. In: IIW/IIS Florence proceedings, IIW Commission XII, Florence, Italia. 2000. p. 1–9.

[13] Rückert G, Huneau B, Marya S. Influence of silica deposit thickness on penetration of GTA welds of austenitic stainless steels. In: ESAFORM 2004 proceedings, Trondheim, Norway. 2004. p. 383–6.